

Available online at [www.sciencedirect.com](http://www.sciencedirect.com)**ScienceDirect**

Procedia Engineering 105 (2015) 576 – 585

**Procedia  
Engineering**[www.elsevier.com/locate/procedia](http://www.elsevier.com/locate/procedia)

6th BSME International Conference on Thermal Engineering (ICTE 2014)

## Numerical study of the wetting and mobility of liquid droplets on horizontal and inclined flat and microgrooved surfaces

Nazia Farhat, Saif Khan Alen, Md. Ashiqur Rahman\*

*Department of Mechanical Engineering, Bangladesh University of Engineering and Technology, Dhaka-1000, Bangladesh*

---

### Abstract

Designing hydrophobic surfaces with controllable wettability has attracted much interest in the recent times. The present study seeks to simulate the static and dynamic wetting behavior of liquid droplets on horizontal flat and microgrooved surfaces and compare the findings with experimentally obtained data. Using an open-source software, a 3D drop-shape model is developed to numerically analyze the shape of liquid droplets and anisotropic wetting for a wide range of parametric space. The effects of droplet volume, variation in the microgroove geometry and wettability gradient along the parallel and perpendicular directions of the microgrooved surfaces *etc.* on the drop shape and apparent contact angle are examined. Simulation and analysis are extended to analyze the wetting behavior of V-grooved geometry and are compared with the findings on rectangular microgrooved surfaces. For creating wettability gradient along the parallel direction of the grooves, periodic PDMS (Polydimethylsiloxane) coating is considered and increased hydrophobicity of the surface is observed with significant increase in the parallel contact angle for this case. The simulated results manifest considerable differences in the wetting pattern of the microgrooved and flat surfaces and are found out to be in good agreement with the experimental findings.

© 2015 The Authors. Published by Elsevier Ltd. This is an open access article under the CC BY-NC-ND license (<http://creativecommons.org/licenses/by-nc-nd/4.0/>).

Peer-review under responsibility of organizing committee of the 6th BSME International Conference on Thermal Engineering (ICTE 2014)

**Keywords:** Wettability; Microgrooved surface; Drop shape modelling; Water retention; Anisotropic wetting.

---

\* Corresponding author. Tel.: +88-01712-274887.

E-mail address: [ashiqurrahman@me.buet.ac.bd](mailto:ashiqurrahman@me.buet.ac.bd)

## 1. Introduction

### Nomenclature

$\theta$	intrinsic contact angle
$\theta_w$	apparent contact angle at Wenzel state
$\theta_c$	apparent contact angle at Cassie state
$r$	roughness factor
$f$	Cassie roughness factor
$\sigma_{sf}$	surface tension at solid-vapor interface
$\sigma_{sl}$	surface tension at solid-liquid interface
$\sigma_{lf}$	surface tension at liquid-vapor interface

Modification of the intrinsic wetting property of metal surfaces can play a significant role in a range of modern technological developments. Analysis of droplet motion and liquid retention property of a surface is important for a wide range of applications such as refrigeration, microfluidic operation, electrowetting-based cooling *etc.* A liquid droplet, when placed on a rough surface, can reside in any of the two different wetting states or modes. The first one is the collapsed state, in which the drop enters into the groove or bottom of the surface roughness and completely wets the substrate. In another mode, the drop forms a composite surface under it. In this composite state, the drop does not enter into the groove, which results into a periodic contact of solid-liquid and liquid-air under the drop. The former collapsed state is termed as 'Wenzel state' and the latter one is called 'Cassie state' of wetting.

Inducing superhydrophobicity in an intrinsically hydrophobic surface is a very active field of research. Many researchers suggested different ways of including roughness to increase the hydrophobic wetting behavior of the surface. In an earlier study, Oliver and Mason [1] reported the influence of surface roughness on the equilibrium spreading of liquids on aluminum and stainless steel surfaces. Bico *et al.* [2] obtained a contact angle close to  $180^\circ$  when they placed a small drop of water on a hydrophobic rough surface. Many researchers modified an intrinsically hydrophobic surface by introducing roughness of different geometry, such as square shaped pillars or rectangular microgrooves to the substrate [3,4]. There has been considerable interest to modify intrinsically hydrophilic surface into hydrophobic surface by introducing roughness. A design and fabrication procedures of such surfaces are described by Cao *et al.* [5], who induced superhydrophobic behavior on hydrophilic surface by micro-texturing the surface. Patankar and He [6,7] in two separate studies, reported hydrophobic behavior on an intrinsically hydrophilic surface by fabricating cavities on the surface and proposed multiple equilibrium droplet shapes on rough hydrophobic surfaces.

Recently, many experimental studies have been reported for analyzing the hydrophobic behavior of intrinsically hydrophilic surface. Abdelsalam *et al.* [8] studied the hydrophobic wetting behavior of regularly structured gold surface, which is hydrophilic in nature. Sommers and Jacobi [9] developed a model for the critical droplet size on microgrooved aluminum surfaces. Rahman and Jacobi [10-14] reported a series of studies on the anisotropic wetting and frosting/defrosting behavior of brass surfaces whose wetting behavior was modified by fabricating rectangular microgrooves on them via micromachining.

Xu and Wang [15], in their study on multi-phase flow on rough hydrophobic surface, derived the Cassie and Wenzel equation from phase field model. Conditions to be satisfied for the wetting transition (Cassie or Wenzel) on rough surfaces were described by several researchers [16-19]. However, these derived conditions were for intrinsically hydrophobic surfaces.

In this present study, a numerical simulation has been conducted to analyze the anisotropic wetting characteristics of brass surfaces with parallel, rectangular microgrooves by varying the geometric properties of the roughness. After validating the numerical results with experimentally obtained data, the simulation is extended to a different groove geometry. Moreover, the effect of periodic wettability gradient, simulating a PDMS coating, along the parallel direction to the groove is analyzed. For this present work, limiting and transition conditions are derived by comparing the Gibb's free energy between the Wenzel and Cassie states. Mathematical condition is given into the simulation software to automatically detect the wetting state of the drop from the given input geometric parameters.

## 2. Numerical simulation

For numerical simulation, Surface Evolver, an interactive software to analyze the liquid drop shape, has been used. Several other researchers [20, 21] used this open access software for numerically simulating and analyzing drop shape and wetting state on different structured surfaces. A detailed description of the simulation procedure is given in the surface evolver manual [22]. A brief explanation of simulation methodology along with the simulation procedure is given in the next section.

### 2.1. Simulation Methodology

For calculating the equilibrium shape of a drop on a substrate, energy minimization needs to be carried out numerically. The total free energy of the system needs to be minimized [20] for obtaining equilibrium drop shape. The free energy  $G$  of the system is expressed as the following equation:

$$G/\sigma_{lf} = A_{lf} - \iint \cos\theta dA \quad (1)$$

where  $\theta$  is the intrinsic contact angle and  $\sigma_{lf}$  are the surface tension at the liquid-air interface. And the integration of the right hand side of this equation is along  $A_{sl}$  which is the area of solid-liquid interface. The intrinsic contact angle can be defined by young's equation:

$$\cos\theta = \frac{\sigma_{sf} - \sigma_{sl}}{\sigma_{lf}} \quad (2)$$

where  $\theta$  is the young's contact angle, and  $\sigma_{sf}$ ,  $\sigma_{sl}$  and  $\sigma_{lf}$  are the interface surface tension at the solid-air, solid-liquid and liquid-air, respectively. In this expression of free energy, the effect of gravity is neglected because in this present work this expression has been used for a small ( $<12 \mu\text{l}$ ) droplets (sessile droplet). For a constant drop volume, the free energy needs to be minimized to obtain the equilibrium drop shape. As the free energy  $G$  is minimized with respect to the liquid-fluid interface shape, it can be observed from equation (1) that the only parameter which contributes to the equilibrium drop shape on a surface is the actual contact angle. Before obtaining the equilibrium shape using free energy minimization, the wetting state of the drop on substrate needs to be defined. Brass is intrinsically hydrophilic ( $\theta < 90^\circ$ ) and in this simulation the wetting state is predicted using the geometry of the microgroove.

### 2.2. Simulation details in Surface Evolver

An open source software 'Surface Evolver' is used to obtain the equilibrium drop shapes. At first the surface is generated by defining its vertices, edges and faces and then geometric, energy and volumetric constraints have been applied to the necessary vertices and edges of the surface. When the droplet is in Wenzel state, the liquid-vapor interface is assumed to have disappeared and the droplet gets the energy corresponding to the intrinsic contact angle of the rough surface locally. When Cassie state is observed, it has been assumed that the liquid-vapor interface at the air-gap gets the liquid-vapor interfacial energy and the contact angle corresponding to this is  $180^\circ$ .

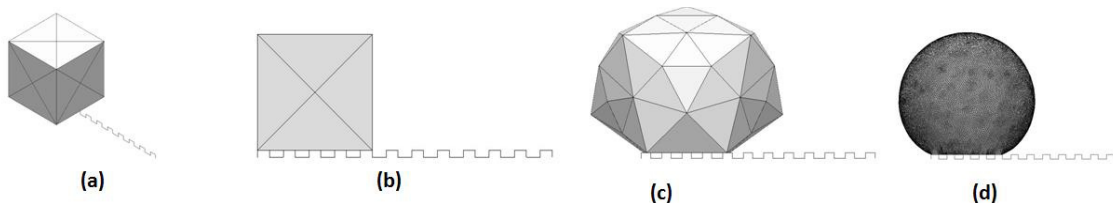


Figure-1: Drop attaining equilibrium shape in simulation (a) Initial Cube on which the constraints are defined (b) Orthogonal view of the initial drop (c) Drop minimizing the surface energy after very small number of iteration (d) Equilibrium drop shape at the end of the simulation.

The drop volume considered in this work is varying between 4  $\mu\text{l}$  to 12  $\mu\text{l}$ , so the effect of gravity can be neglected as the drop radius  $R$  is less than the capillary length  $\alpha$  and so the liquid-vapor interface at the groove can be taken as a straight line instead of a curvature. Here  $\alpha$  is defined as

$$\alpha = \sqrt{\frac{\sigma(lf)}{\Delta\rho g}} \quad (3)$$

where  $\sigma_{lf}$  is the surface tension in solid-air interface and  $\Delta\rho$  is the difference between liquid density and the density of the surrounding air.

Among the four edges of the bottom face, left and right edges are constrained to move on two outer most pillars respectively. This boundary condition is necessary because physically the number of pillar on which the drop resides is defined by the drop formation process. While applying the constraints to the facets and edges in the simulation, only the bottom face is considered to be responsible for obtaining the shape of the droplets. For convenience, the boundary conditions are given to the edges, which contribute to generate the three phase contact line. Figure 1 illustrates the steps involved in the simulation in Surface Evolver. As we can see from Figure 1(c), after a small number of iterations, droplet tries to obtain a minimum energy (spherical) shape. After sufficient iterations and several refinement steps, the droplet finally attains the required spherical shape as shown in Figure 1(d).

### 3. Result analysis and discussion

#### 3.1. Sample geometry and contact angle data

For the present work, eight microgrooved brass samples with four having a constant groove depth and width and four more samples with a constant groove width and pillar width are selected for drop shape analysis and simulation. To verify the validity of the numerical simulation, the experimentally and numerically obtained orthogonal and parallel contact angles and shape of the droplets under the same conditions are compared.

In order to ensure that the comparisons are made for the same conditions, all parameters (droplet size, number of pillars the experimental and simulated drops are resting on, dimension of the groove geometry parameters such as width, depth and spacing *etc.*) are kept constant. Topographic data of all the rectangular microgrooved brass samples used in the present study and experimentally and numerically observed wetting state on different surfaces (rectangular and V-grooved surfaces, surfaces with imposed wettability gradient) are shown in Table 1. All the microgrooved samples had a fixed groove width of 130  $\mu\text{m}$ . The number of pillars the liquid drops are resting on for different surfaces, along with the contact angle data obtained experimentally and from simulation, are for a fixed drop volume of 5  $\mu\text{l}$ .

Table-1: Topographic data 8 microgrooved brass samples used in this present study. The microgrooved samples are designated as  $D_G^x W_P^y W_G^z$ ; where  $D_G$ ,  $W_P$ ,  $W_G$  stand for the groove depth, pillar width, and groove width, respectively, and the superscripts  $x$ ,  $y$  and  $z$  represent the numerical values of these parameters.

Sample	Dimensions ( $\mu\text{m}$ )			Wetting State			
	Depth of Groove (Dg)	Width of Pillar (Wp)	Width of Groove (Wg)	Experimental	Rectangular Groove	V Groove	Rectangular Groove With Wettability Gradient
$D_G^{67} W_P^{26} W_G^{130}$	67	26	130	Wenzel	Wenzel	Wenzel	Wenzel
$D_G^{67} W_P^{80} W_G^{130}$		80		Cassie	Cassie	Wenzel	Cassie
$D_G^{67} W_P^{110} W_G^{130}$		110		Cassie	Cassie	Wenzel	Cassie
$D_G^{67} W_P^{187} W_G^{130}$		187		Cassie	Cassie	Wenzel	Cassie
$D_G^{27} W_P^{112} W_G^{130}$	27	112	130	Wenzel	Wenzel	Wenzel	Wenzel
$D_G^{67} W_P^{112} W_G^{130}$	67			Cassie	Cassie	Wenzel	Cassie
$D_G^{98} W_P^{112} W_G^{130}$	98			Cassie	Cassie	Wenzel	Cassie
$D_G^{122} W_P^{112} W_G^{130}$	122			Wenzel	Wenzel	Cassie	Wenzel

Table-2: Comparison of numerically obtained apparent contact angle data with experimental results of 8 microgrooved brass samples (constant drop volume of 5  $\mu$ l and number of pillar is selected from the experimental observation)

Sample	Volume of Water Droplet (ul)	No. of Pillars Under the Droplet	Experimentally Measured Contact Angle (°)		Numerically Obtained Contact Angle (°)	
			Orthogonal	Parallel	Rectangular Groove	
					Orthogonal	Parallel
$D_G^{67}W_P^{26}W_G^{130}$	5	10	141.6	53.1	131.6	60.8
$D_G^{67}W_P^{80}W_G^{130}$	5	6	144.9	124.0	153.4	123.7
$D_G^{67}W_P^{110}W_G^{130}$	5	5	145.7	85.2	150.6	90.0
$D_G^{67}W_P^{187}W_G^{130}$	5	4	142.9	115.5	148.2	90.0
$D_G^{27}W_P^{112}W_G^{130}$	5	6	134.7	63.4	134.1	61.1
$D_G^{67}W_P^{112}W_G^{130}$	5	5	145.7	85.2	150.6	90.0
$D_G^{98}W_P^{112}W_G^{130}$	5	5	142.8	100.3	150.4	92.0
$D_G^{122}W_P^{112}W_G^{130}$	5	5	132.7	27.3	138.6	51.3

### 3.2. Comparison and analysis of the experimental and numerical results

One of the primary objectives of this work was to examine the effect of roughness geometry on the wettability of a surface. The key parameters when analyzing the wetting behavior of a surface are the wetting state and apparent contact angle. The apparent contact angle in the orthogonal direction of the grooves is also considerably dependent on the number of pillar rather than the dimension of the roughness. So when wetting state is defined, parallel contact angle is the only parameter that plays an important role to compare wetting behavior of two surfaces. So to investigate the wetting behavior of different roughness geometry, at first the numerical results and experimental findings of rectangular microgroove surface were compared in Figures 2(a-d). The experimental values had an uncertainty of  $\pm 4^\circ$ , and the numerical results agreed with the experimental one with a maximum difference of  $\pm 10^\circ$ .

It should be noted here that the simulation conditions for obtaining the numerical results of Figure 2 were very realistic as they were for the same geometry, same drop size and rested on the same number of pillars as that of the experiments. An excellent agreement between the numerical and experimental findings can be observed from Figure 2 for a fixed drop volume of 5  $\mu$ l. It means that the simulations were successful in capturing the wetting physics properly. Also the wetting state was successfully captured with the given input conditions which were derived mathematically by using energy balance between Cassie and Wenzel states. Next, the validity of this simulation procedure was examined further for random size of the droplets and similar set of simulations were performed by varying the droplet volume from 4  $\mu$ l to 12  $\mu$ l and choosing experimentally validated supporting pillar numbers for a particular liquid drop. The results are plotted in Figures 3(a-d), from where it can be clearly seen that the findings exhibit very similar trend and the experimental and numerical values vary within a range of  $15^\circ$ . But in some cases the differences were significant in the parallel direction and especially for the droplets in a Wenzel wetting state. It is because the software is not able to include the physics of capillary channeling, which causes the droplet to expand significantly along the grooves in Wenzel wetting, especially observed for machined grooves [1,10].

Now that a good agreement between the numerical results and experimental findings is obtained, our study is extended to examine the wetting behavior of this rough brass surfaces with different roughness geometry. For this, the simulation was conducted for V-grooved brass surfaces with similar dimensions (groove depth and groove width at the top) of rectangular grooves. And it can be seen clearly from Figure 4(b) that for all 8 microgrooved brass surfaces, V-grooved geometry demonstrates a parallel contact angle of  $55^\circ$ - $60^\circ$ , which were much less than that of surfaces with rectangular grooves under the same conditions. The reason behind this is that a V-grooved surface has a lower droplet suspending ability than that of a rectangular grooved surface. As a result, the wetting state was Wenzel, resulting in a significant decrease in the parallel contact angle. Therefore, replacing the rectangular grooves with V-grooves is unlikely to increase the hydrophobicity, though machining a V-grooved surface is easier than machining a rectangular grooved surface.

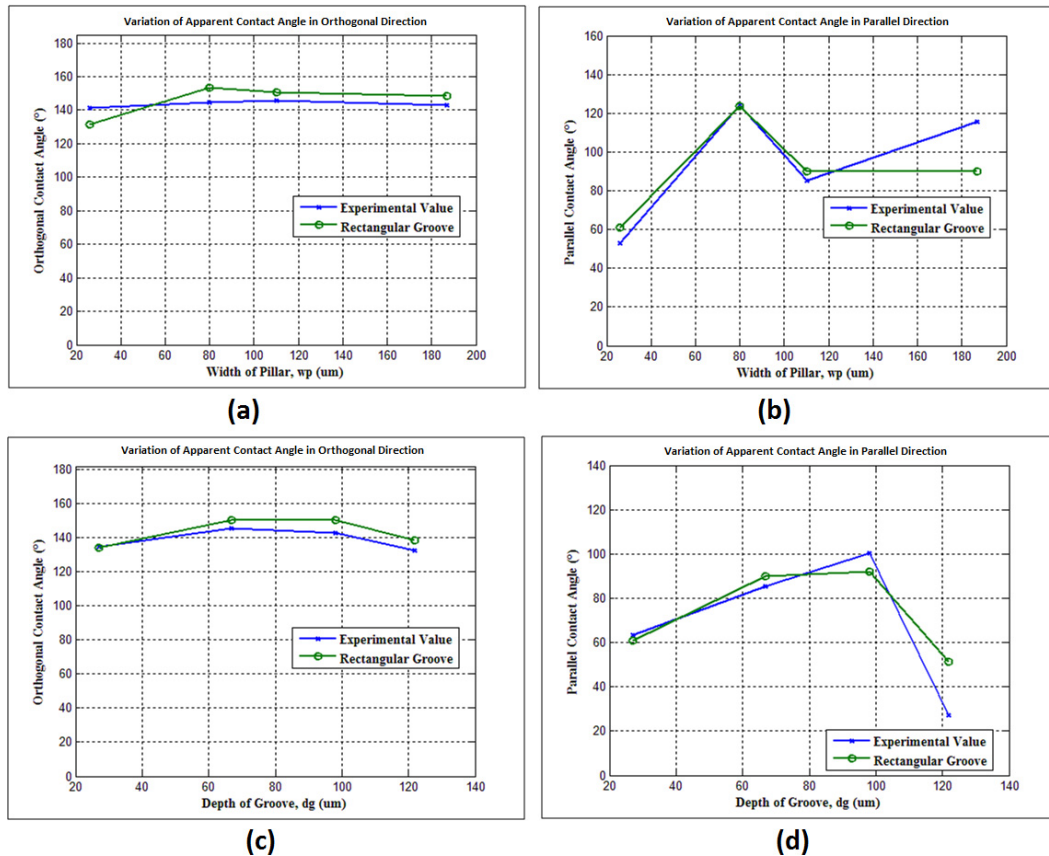


Figure-2: Comparison between experimental and numerically obtained results for surfaces with a variation of pillar width (top row) and groove depth (bottom row), keeping all other parameters constant (for drop volume= 5  $\mu$ l). These variation are shown for apparent contact angles along the (a) orthogonal direction with varying  $W_p$  ( $D_g=67$   $\mu$ m,  $W_g=130$   $\mu$ m) (b) parallel direction with varying  $W_p$  ( $D_g=67$   $\mu$ m,  $W_g=130$   $\mu$ m) (c) orthogonal direction with varying  $D_g$  ( $W_p=112$   $\mu$ m,  $W_g=130$   $\mu$ m), and (d) parallel direction with varying  $D_g$  ( $W_p=112$   $\mu$ m,  $W_g=130$   $\mu$ m).

Since the consideration of V-grooved geometry did not provide a possible solution for obtaining a more hydrophobic behavior of the surface, the simulation was further extended for rectangular microgrooved surface which has periodic wettability gradient on the pillars. The concept of providing a periodic wettability gradient along the parallel direction to the groove simulated the physical condition of coating the surface periodically with strips of PDMS (Polydimethylsiloxane) 200  $\mu$ m wide with a gap of 200  $\mu$ m across the pillars. When this wettability gradient was applied, a significant rise in parallel contact angle can be observed from Figure 4 (b,d). A new composite surface of brass and PDMS under the drop on the pillar may be responsible for this significant rise. For sample  $D_g^{67}W_p^{112}W_g^{130}$ , this increase in parallel contact angle was 22°. And for every sample, applying wettability gradient increased the contact angle in the parallel direction of the grooves by almost 20°, which might promote a better water drainage behavior of the surface.

### 3.3. Drop shape comparison

Comparison between the numerical result and experimental drop shape enables to obtain a proper validation of the simulation methodology. In the present study, a close agreement between the experimental and the simulated drop shapes on rectangular microgroove surfaces was observed. It was observed from the simulation that the pillar number has a significant effect on the orthogonal contact angle. Therefore, the number of pillars along with the other



groove dimensions was kept constant to systematically analyze the variation in the wetting behavior among rectangular groove, V-groove, and periodically wettability gradient surfaces.

The top views of liquid droplet from both experimental and numerical results are compared in Figure 5. From Figures 5(a,b), we can see that for sample  $D_G^{122}W_P^{112}W_G^{130}$  that the shape of the water droplets obtained experimentally and from our simulation exhibited excellent agreement. The drop shape was elliptical due to the fact that the wetting state for this sample was Wenzel. So the parallel contact angle was much less than the orthogonal contact angle, resulting in an elliptical drop shape. From this top view comparison, the small deviation from the experimental shape may be seen which was probably due to the fact that the experimental drop shape was for a drop size of  $25\text{ }\mu\text{l}$  while the simulation result is for a  $10\text{ }\mu\text{l}$  drop. From Figures 5(c, d) it can be seen that the three-phase contact angle for the sample of  $D_G^{67}W_P^{110}W_G^{130}$  ( $5\mu\text{l}$ ) was not a regular ellipse. Some portion of this three-phase contact line was irregular along the orthogonal direction to the groove. The main reason behind this was that sample  $D_G^{67}W_P^{110}W_G^{130}$  formed a Cassie (composite) state over the substrate. As a result a composite state of solid-liquid and solid-air contact line was formed. Similar findings were reported by Patankar *et al.* [20].

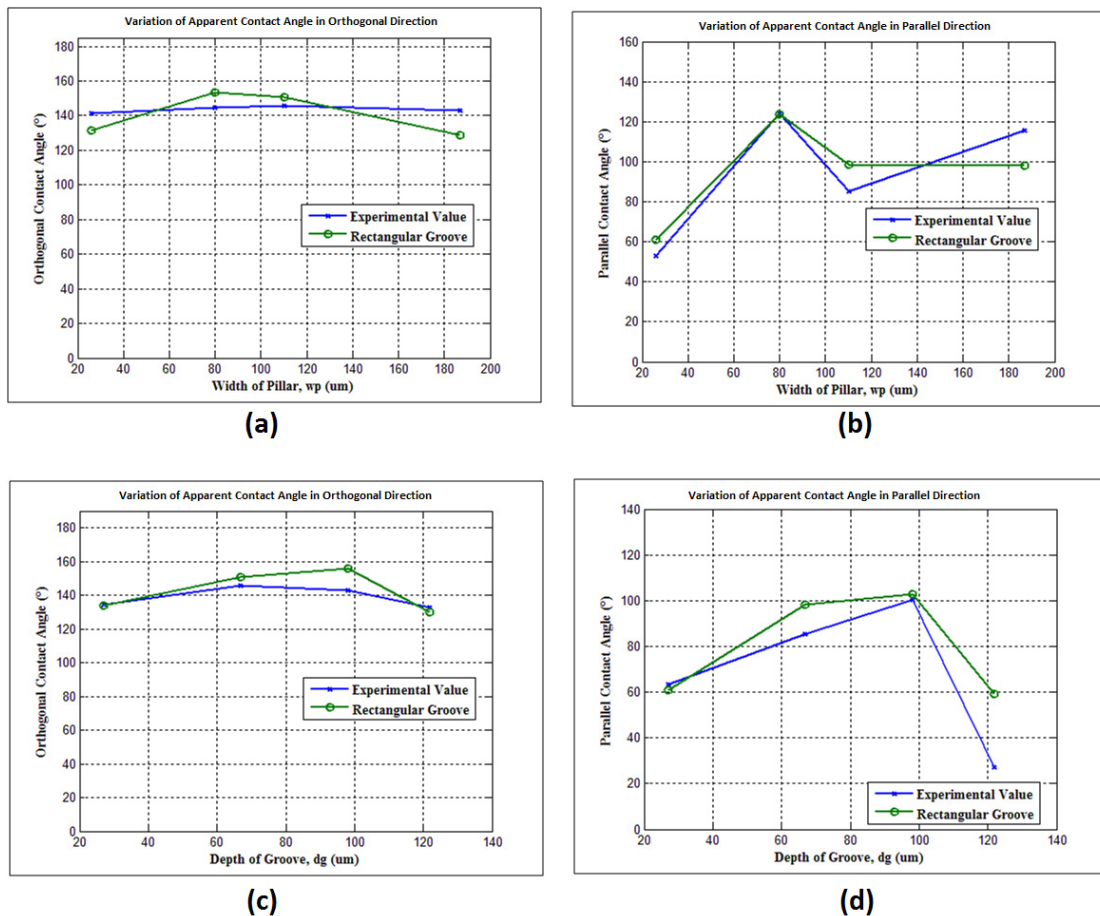


Figure-3: Comparison between experimental and numerically obtained results for surfaces with a variation of pillar width (top row) and groove depth (bottom row), for different combinations of drop volume ( $4\text{ }\mu\text{l}$  -  $12\text{ }\mu\text{l}$ ) and experimentally validated number of pillars supporting the droplets. These variations are shown for apparent contact angles along the (a) orthogonal direction with varying  $W_P$  ( $D_G=67\text{ }\mu\text{m}$ ,  $W_G=130\text{ }\mu\text{m}$ ) (b) parallel direction with varying  $W_P$  ( $D_G=67\text{ }\mu\text{m}$ ,  $W_G=130\text{ }\mu\text{m}$ ) (c) orthogonal direction with varying  $D_G$  ( $W_P=112\text{ }\mu\text{m}$ ,  $W_G=130\text{ }\mu\text{m}$ ), and (d) parallel direction with varying  $D_G$  ( $W_P=112\text{ }\mu\text{m}$ ,  $W_G=130\text{ }\mu\text{m}$ ).

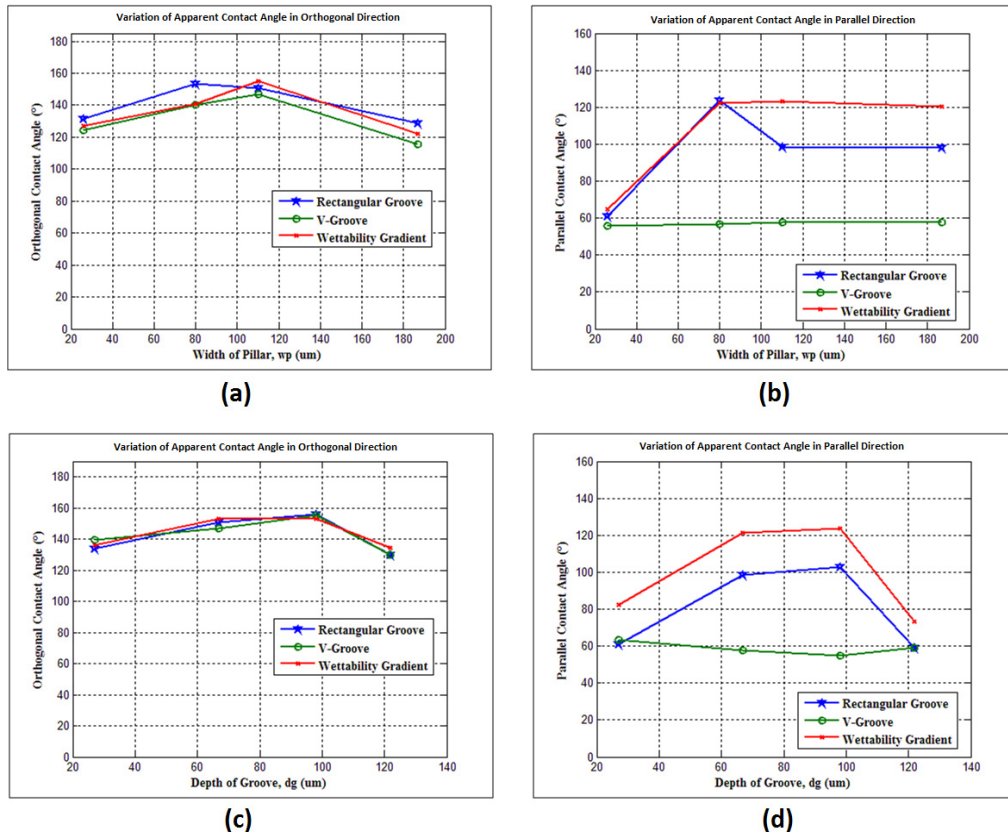


Figure-4: Comparison among numerically obtained contact angles for surfaces with rectangular grooves, V-grooves and rectangular grooves with an imposed wettability gradient. Plot is obtained by changing the width of pillar and depth of groove successively, for different combination of drop volume (4 -12  $\mu\text{l}$ ) and experimentally validated number of pillars. The results are shown for apparent contact angles along the (a) orthogonal direction with varying  $W_p$  ( $D_G=67$   $\mu\text{m}$ ,  $W_G=130$   $\mu\text{m}$ ) (b) parallel direction with varying  $W_p$  ( $D_G=67$   $\mu\text{m}$ ,  $W_G=130$   $\mu\text{m}$ ) (c) orthogonal direction with varying  $D_G$  ( $W_F=112$   $\mu\text{m}$ ,  $W_G=130$   $\mu\text{m}$ ), and (d) parallel direction with varying  $D_G$  ( $W_F=112$   $\mu\text{m}$ ,  $W_G=130$   $\mu\text{m}$ ).

To compare the drop shape along the orthogonal and parallel direction to the groove, samples  $D_G^{67}W_p^{26}W_G^{130}$  and  $D_G^{67}W_p^{187}W_G^{130}$  were selected, which exhibited a Wenzel and Cassie wetting state, respectively. From Figures 6-7, it can be seen clearly that the simulation software could accurately sense the wetting state of the drop and at the same time accurately captured the wetting dynamics. The shape of the droplet from both the orthogonal and parallel directions of the grooves obtained experimentally and numerically matched very closely as we can see from Figures 6(a,b) and Figures 6(e,f), respectively. From Figures 6(f,g), it can be seen that in case of a V-grooved surface, the parallel contact angle remained nearly same as the wetting state in this case was Wenzel for both the rectangular and V-grooved surfaces. In addition, Figures 6(f,h) clearly indicates that an imposed wettability gradient (a 200  $\mu\text{m}$  strip simulating PDMS coating which has a contact angle of 114° and applied periodically with a spacing of 200  $\mu\text{m}$ ) increased the contact angle, especially in the parallel direction of the groove. There was a maximum of 20° increase in parallel contact angle for this wettability gradient condition. The modified wettability obtained by incorporating a wettability gradient may be used further for obtaining better water drainage behavior from microgrooved surfaces.

From Figure 7, a similar analysis may be performed while comparing the drop shapes for different groove geometry which exhibited a Cassie wetting state experimentally. Here, from Figure 7(g), it can be seen that the contact angle decreased considerably on the V-grooved surface. It was because of the difference in wetting states (Cassie and Wenzel) between rectangular and V-grooved surfaces having the same groove dimensions. From the excellent agreement between the experimental and rectangular microgrooved drop shapes, it is obvious that the developed software for this numerical simulation is capturing the wetting physics accurately.



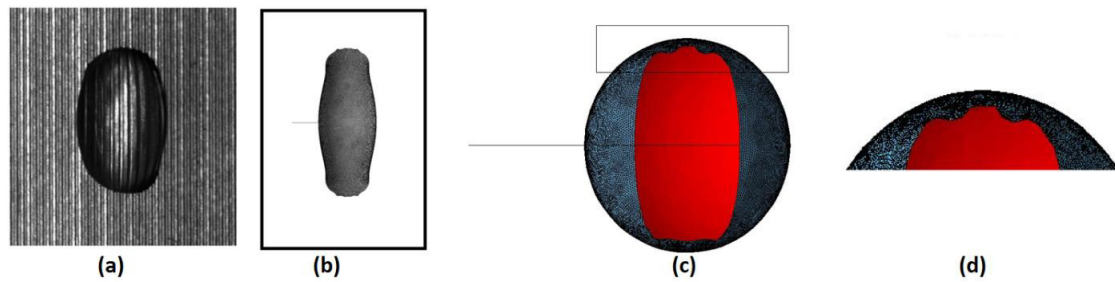


Figure-5: Top view of a water droplet on rectangular microgrooved sample  $D_G^{122}W_P^{112}W_G^{130}$  (a) Experimental result (b) From Simulation. And bottom view of the drop sample  $D_G^{67}W_P^{110}W_G^{130}$  from numerical simulation on rectangular microgrooved surface to analysis of three phase contact line (c) Original view (d) Magnified view of the selected portion.

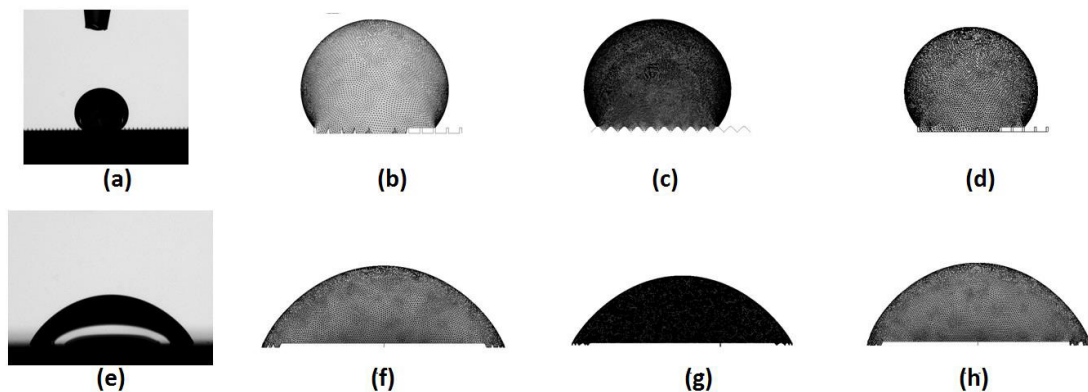


Figure-6: Drop Shape for sample  $D_G^{67}W_P^{26}W_G^{130}$  (5  $\mu$ l drop volume residing on 10 pillars) viewed from both orthogonal and parallel direction of the grooves. In the top row, drop shape from the orthogonal direction obtained from (a) Experiments (b) Simulation (rectangular groove) (c) Simulation (V-groove) and (d) Simulation (rectangular groove with wettability gradient). In the bottom row (e-h), drop shape from the parallel direction of the grooves on these surfaces in the same order.

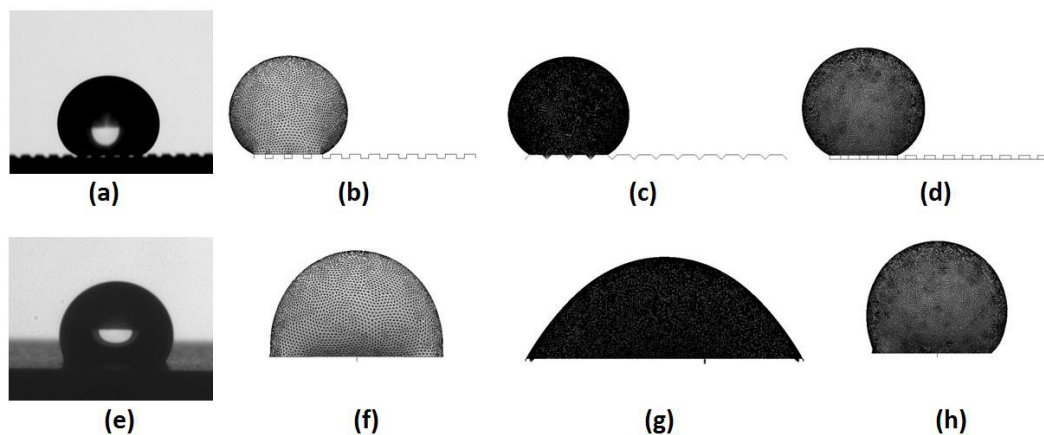


Figure-7: Drop Shape for sample  $D_G^{67}W_P^{187}W_G^{130}$  (5  $\mu$ l drop volume residing on 4 pillars) viewed from both orthogonal and parallel direction of the grooves. In the top row, drop shape from the orthogonal direction obtained from (a) Experiments (b) Simulation (rectangular groove) (c) Simulation (V-groove) and (d) Simulation (rectangular groove with wettability gradient). In the bottom row (e-h), drop shape from the parallel direction of the grooves on these surfaces in the same order.

#### 4. Conclusion

A detailed numerical simulation was been performed to analyze the wetting behavior of microgrooved brass surfaces having a variation of groove depth and spacing. The main objective of this work was to capture the wetting state and wetting dynamics accurately on these surfaces, along with the same on other designed micro structured surfaces. Drop shape analysis was performed and compared for the experimental and numerical results for a total of 8 microgrooved surfaces. Experimental findings and numerical results showed a very good agreement, with a maximum variation of less than  $\pm 10^\circ$ . The simulation was then extended further for V-grooved surfaces with similar groove dimension as that of rectangular microgrooves. However, no significant improvement in the wetting behavior of the brass surfaces were observed, rather the contact angles in the parallel direction of the grooves were found to decrease on V-grooved surfaces due to the wetting state being Wenzel for the same groove depth and width. On the contrary, applying a periodic wettability gradient simulating 200  $\mu\text{m}$  PDMS strips on the pillars along the parallel direction to the groove significantly altered the wetting behavior of the surface. The increase in contact angle in the parallel direction of the microgrooves due to the imposed wettability gradient was as high as  $20^\circ$ . The authors are working now to develop a mathematical model that can predict the wetting state of the liquid droplet from the roughness geometry of a rough hydrophobic surface having an intrinsically hydrophilic behavior.

#### Reference

- [1] J. F. Olivier, S. G. Mason, Liquid spreading on rough metal surfaces, *Journal of Material Science* 15 (1980), pp. 431-437.
- [2] J. Bico, C. Marzolin, D. Quere, Pearl drops, *Europhysics Letters* 47 (2) (1999), pp. 220-226.
- [3] N. A. Patankar, On the Modeling of Hydrophobic Contact Angles on Rough Surfaces, *Langmuir* 2003, 19, pp. 1249-1253.
- [4] L. Barbieri, Wetting properties of flat-top periodically structured superhydrophobic surfaces, The University of Genoa, Italy.
- [5] L. Cao, H. H. Hu, D. Gao, Design and Fabrication of Micro-textures for Inducing a Superhydrophobic Behavior on Hydrophilic Materials, *Langmuir*, 2007.
- [6] B. He, N. A. Patankar, J. Lee, Multiple Equilibrium Droplet Shapes and Design Criterion for Rough Hydrophobic Surfaces, *Langmuir*, 2003.
- [7] N. A. Patankar, Hydrophobicity of Surfaces with Cavities: Making Hydrophobic Substrates from Hydrophilic Materials?, *Journal of Adhesion Science and Technology*, April, 2012.
- [8] M. E. Abdelsalam, P. N. Bartlett, T. Kelf, Jeremy Baumberg, Wetting of Regularly Structured Gold Surfaces, *Langmuir*, 2005, 21, pp. 1753-1757.
- [9] A. D. Sommers, A. M. Jacobi, Wetting phenomenon on micro-grooved aluminum surfaces and modeling of the critical droplet size, *Journal of Colloid and Interface Science*, 2008.
- [10] M. A. Rahman, A. M. Jacobi, Wetting Behavior and Drainage of Water Droplets on Microgrooved Brass Surfaces, *Langmuir*, 2012.
- [11] M. A. Rahman, A. M. Jacobi, Study of frost properties and frost melt water drainage on microgrooved brass surfaces in multiple frost/thaw/refrost cycles, *Applied Thermal Engineering*, 2014.
- [12] M. A. Rahman, A. M. Jacobi, Effect of microgroove geometry on the early stages of frost formation and frost properties, *Applied Thermal Engineering* 56 (2013), pp. 91-100.
- [13] M. A. Rahman, A. M. Jacobi, Experimental study on condensation, frost formation and condensate retention on microgrooved and plain brass surfaces under natural convection condition, 8th International Conference on Heat Transfer, Fluid Mechanics and Thermodynamics, 26th June - 1st July 2011, Pointe Aux Piments, Mauritius.
- [14] M. A. Rahman, A. M. Jacobi, Drainage of frost melt water from vertical brass surfaces with parallel microgrooves, *International Journal of Heat and Mass Transfer* 55 (2012), pp. 1596-1605.
- [15] X. Xu, X. Wang, Derivation of the Wenzel and Cassie equations from phase field model for two phase flow on rough surface, *SIAM J. Appl. Math.*, Vol. 70, No. 8, pp. 2929-2941.
- [16] E. Bormashenko, Progress in understanding wetting transitions on rough surfaces, *Advances in Colloid and Interface Science*- 2014.
- [17] C. X. Ling, L. Tian, The apparent state of droplets on a rough surface, *Science in China Series G: Physics, Mechanics & Astronomy*- 2009.
- [18] E. Bormashenko, Wetting transitions on biomimetic surfaces, *Phil. Trans. R. Soc. A*- 2010.
- [19] X. Cui, W. Li, On the possibility of superhydrophobic behavior for hydrophilic materials, *Journal of Colloid and Interface Science*- 2010.
- [20] Y. Chen, B. He, J. Lee, N. A. Patankar, Anisotropy in the wetting of rough surfaces, *Journal of Colloid and Interface Science* 281 (2005), pp. 458-464.
- [21] N. Janardan, M. V. Panchagnula, Effect of the initial conditions on the onset of motion in sessile drops on tilted plates, *Colloids and Surfaces A: Physicochemical and Engineering Aspects*, 2014.
- [22] K. A. Brakke, <http://www.susqu.edu/facstaff/b/brakke/evolver>.